Journal of Tissues and Materials

Physical Evaluation of 3D-Printed Gelatin-hydroxyapatite-reduced Graphene Oxide Nanocomposite as a Bone Tissue Engineering Scaffold

Hassan Nosrati[1], **Rasoul Sarraf-Mamoory**[*1], **Dang Quang Svend Le**[2], **Maria Canillas Perez**[3], **Cody Eric Bünger**[*2]

[1]Department of Materials Engineering, Tarbiat Modares University, Tehran, Iran.
[2]Department of Clinical Medicine, Aarhus University, Denmark.
[3]Instituto de Cerámica y Vidrio, CSIC, Madrid, Spain.

* Correspondence to: Sarraf-Mamoory R. (E-mail: rsarrafm@modares.ac.ir)
* Correspondence to: Bünger C.E. (E-mail: codybung@rm.dk)

Abstract

Introduction: Hydroxyapatite (HA) and graphene have recently been added to gelatin as reinforcing phases (individually or together). These materials increase the mechanical and biological properties of gelatin and extend gelatin applications as tissue engineering scaffolds.

Objective: In this study, the physical properties of these scaffolds were evaluated using scanning electron microscopy by detail.

Material and Methods: A hydrogel 3D-printing method and freeze drying were used in this study. The analysis performed in the sample includes X-ray diffraction, Scanning Electron Microscope, and bending.

Result: The findings of this study showed that the addition of graphene and HA to gelatin changed the rheology, reduced the size of pores, and increased the accuracy of the designed pores. The addition of HA and graphene also increased the bending strength and changed the shape of the resulting cracks.

Conclusion: The findings of this study will be useful for the design of tissue engineering scaffolds.

Keyword: Hydroxyapatite; Graphene; Scaffold; Gelatin; 3D-Printing

Received: 3 January 2020, **Accepted**:3 March 2020

DOI: 10.22034/jtm.2020.218433.1024

Tissues & Biomaterials Research Group

1. Introduction

Graphene with the honeycomb structure, the thickness of a carbon atom, and excellent mechanical properties have received much attention in recent years [1-4]. Graphene is a member of the carbon nanomaterials (carbon nanotubes, graphene, and nanodiamond) family, but its high specific surface area has made graphene sheets highly reinforcing [5]. Therefore, graphene has been extensively investigated in nanocomposite applications. Due to the biocompatibility of graphene, it has found wide applications in the medical field, including drug delivery, orthopedics, and bioimaging [6-9]. It has been used as a reinforcing phase in addition to HA. HA-graphene nanocomposites have the potential to be used in orthopedics as bone replacement implants. HA is very similar to the bone mineral and is less soluble in biological environments than other calcium phosphates. HA has a hexagonal crystalline structure and its unique biological properties make it one of the most widely used bioseramics [10-13]. Addition of graphene can improve the mechanical weakness of HA somewhat. A variety of methods have been used for the synthesis of ceramics, such as sol-gel and hydrothermal [14-17]. Like other ceramics, HA is synthesized in a variety of ways, including combustion preparation [18], solid-state reaction [19], electrochemical deposition [20], sol-gel [21, 22], hydrolysis [23], precipitation [24, 25], sputtering [26], multiple emulsion [27], biomimetic deposition [28], solvothermal method [29], and hydrothermal process [30]. Among these methods, hydrothermal process is more important than other methods due to its high control, high crystallinity, and variability in morphology. The use of hydrothermal method is also suitable for the synthesis of graphene-HA hybrid powders as it does not require calcination. Also, since the hydrothermal process is an in situ method, the quality of the hybrid powder is better than the mechanical blending methods [31-34].

HA and graphene have recently been added to gelatin as reinforcing phases (individually or together). These materials increase the mechanical and biological properties of gelatin and extend gelatin applications as tissue engineering scaffolds. In particular, with the advent of advanced technologies such as 3D-printing, gelatin applications have increased dramatically. Gelatin has excellent printability and because the resulting gel is well blended with graphene-HA powders, it is possible to fabricate complex shapes using 3D-printing with gel containing HA and graphene sheets. In one published study, gelatin-graphene-HA nanocomposites were fabricated by 3D-printing method. The HA-graphene powders used as reinforcing phase were synthesized using the hydrogen gas injected hydrothermal process. Some evaluations of powders and scaffolds have already been published [35]. In this study, the physical properties of these scaffolds were evaluated using scanning electron microscopy by detail.

2. Experimental

The gels used for 3D-printing were prepared according to Table 1. The method of preparing these gels has already been published [35]. Figure 1 shows the gels used for 3D-printing, 3D-printing set up, and freeze dried scaffolds. Pure gelatin, gelatin-HA, gelatin-HA-rGO scaffolds were fabricated by a hydrogel 3D-printing system connected to a 3D robot. The hydrogels were put in an oven (65 ^{o}C) and stirred for 12 h. The working bed temperature was -10 ^{o}C and the heating barrel fixed to the 3D-printer was set to 40^{o}C. A 200 μm needle tip moving at a speed of 30 mm s^{-1} was used to extrude the hydrogels. The solution blend was laid by varying the air pressures. The printed scaffolds subsequently were put in a freeze dryer (- 60 ^{o}C) for 72 h [35]. The scaffolds were printed in 3 cm x 3 cm dimensions and circled using a punch.

The characterization methods and softwares used in this study with the specifications are listed in Table 2.

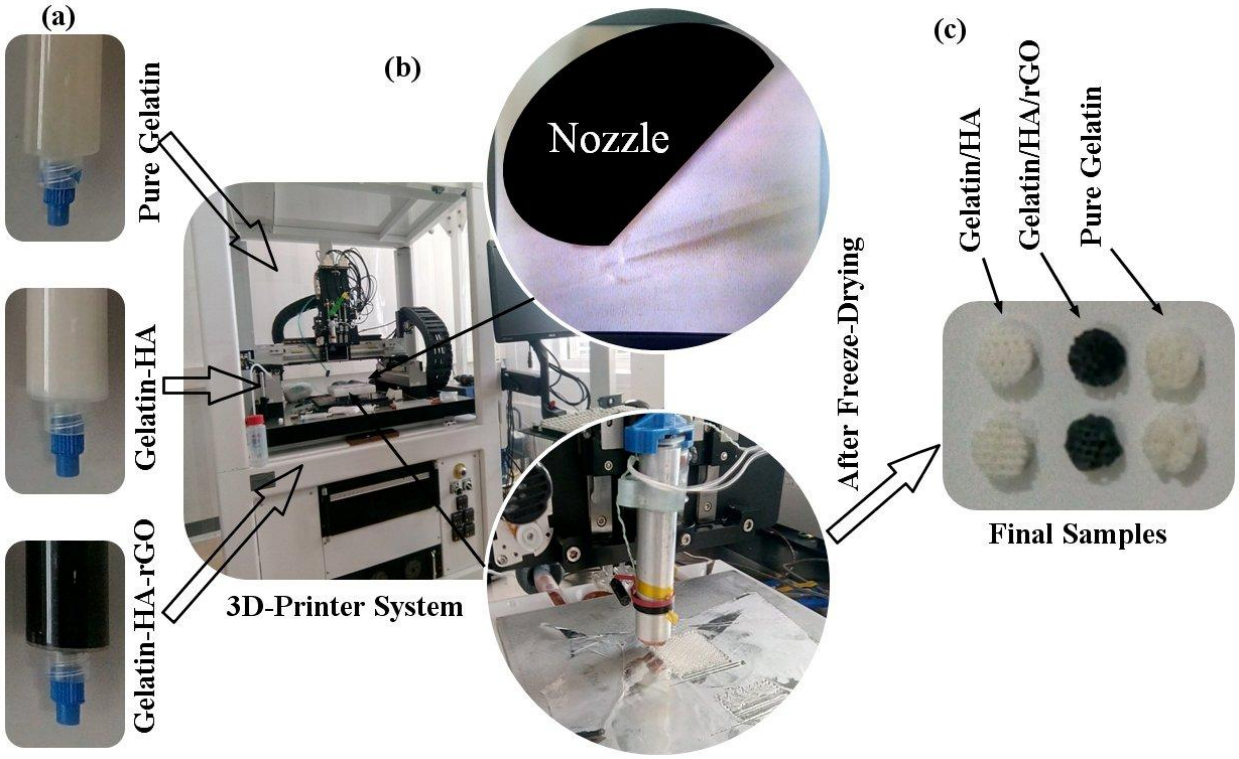

Figure 1: (a) the gels used for 3D-printing, (b) 3D-printing set up, (s) printed and freeze dried scaffold

Table 1: 3D-printed scaffolds specification

Scaffold	Gelatin/7 cm^3 Water	rGO	HA
Pure Gelatin	3 gr	0	0
Gelatin-HA	2.7 gr	0	0.3 gr
Gelatin-HA-rGO	2.7 gr	0.0045 gr	0.2955 gr

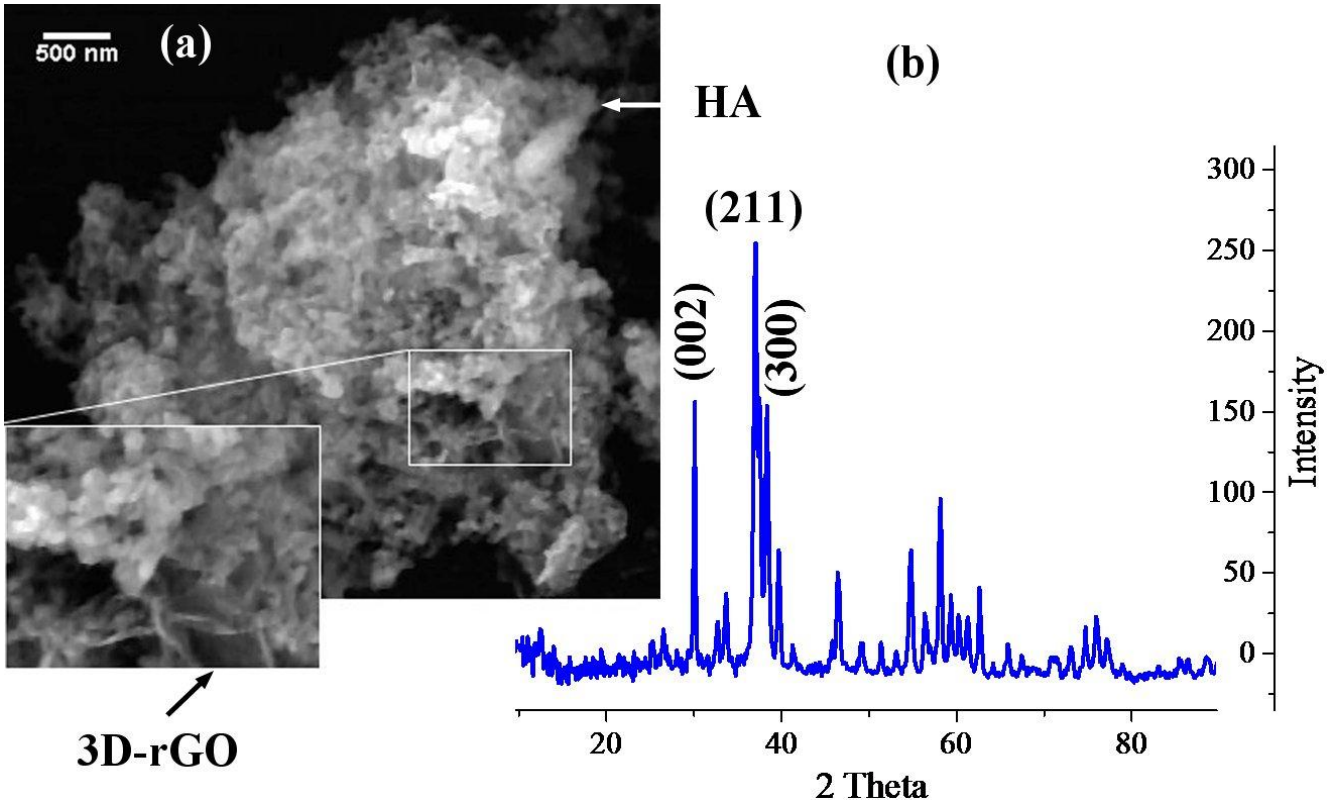

Figure 2: (a) FESEM image of graphene-HA powders, (b) XRD pattern of graphene-HA powders

Table 2: The characterization methods used in this study

Analysis Method	Instrument Specification
XRD	X' Pert Pro, Panalytical Co.
FESEM	Hitachi S4700
Diamond	3.2 (version)
Origin pro	2016

3. Results and discussion

Figure 2 shows the FESEM image and the XRD pattern of graphene-HA powders. As can be seen in the FESEM image, the powders contain HA and graphene. Graphene sheets are interconnected and form a three-dimensional structure. But the XRD pattern of these powders is consistent with the pure HA pattern and the graphene peaks are covered by the HA peaks. The main growth planes of HA crystals consist of (002), (211), and (300). The HA used in this study are nano-rods grown in the direction of (002) planes (c axis) [36-38].

Figure 3 shows the FESEM images of pure gelatin scaffold, gelatin molecule structure, and pure gelatin scaffold photo. The pores in these scaffolds are spherical. The pores are less than 30 micrometer in size. These porosities have created a three-dimensional structure with closed porosities. There are two types of porosity in these scaffolds. One is 300 micrometer designed porosity and the other is a 30 micrometer small porosity [35].

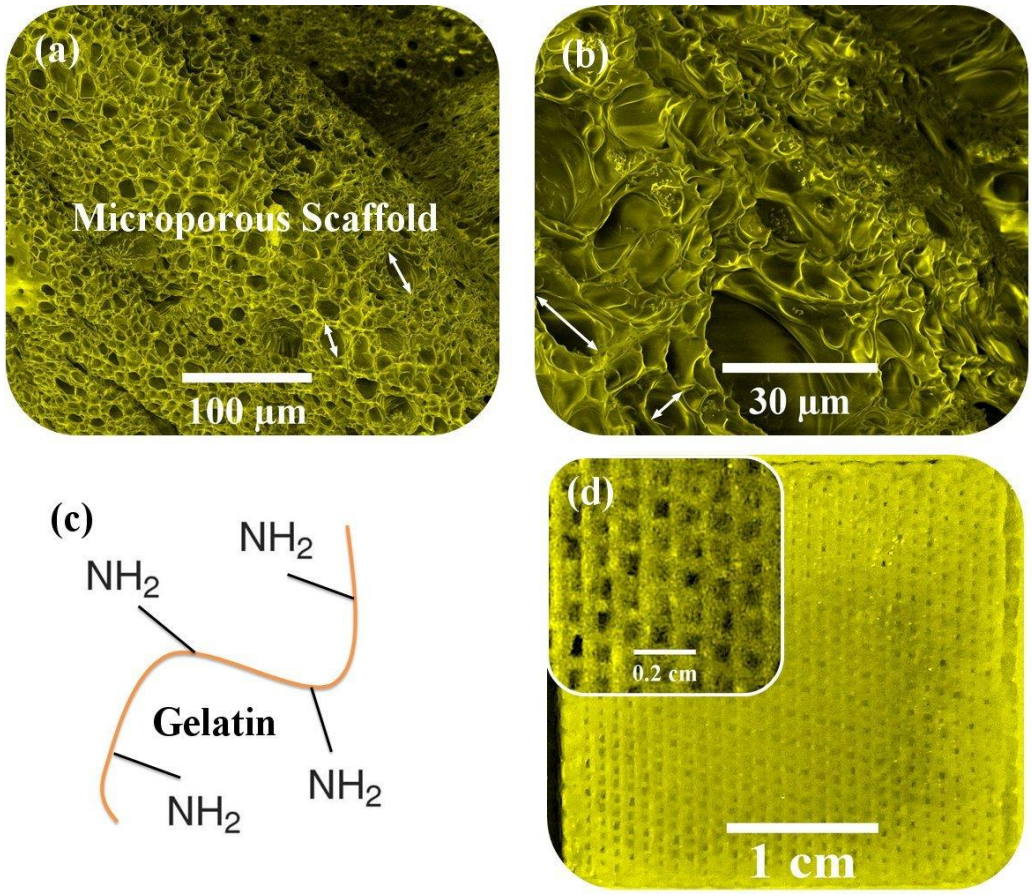

Figure 3: (a, b) FESEM images of pure gelatin scaffold, (c) gelatin molecule structure, (d) pure gelatin scaffold photo

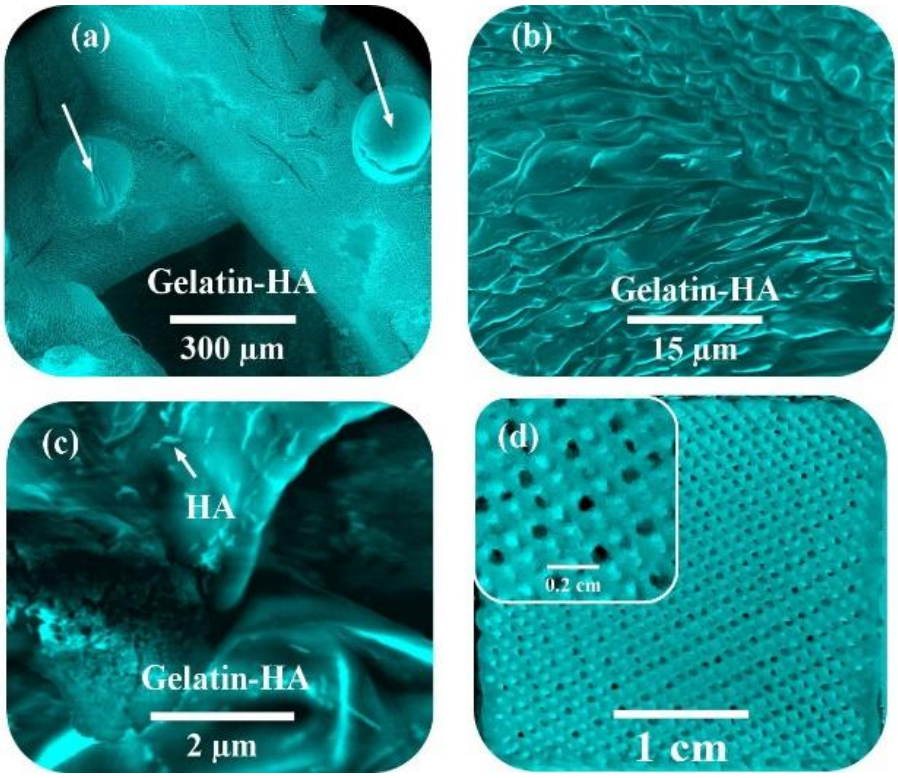

Figure 4: (a-c) FESEM images of gelatin-HA scaffold, (d) gelatin-HA scaffold photo

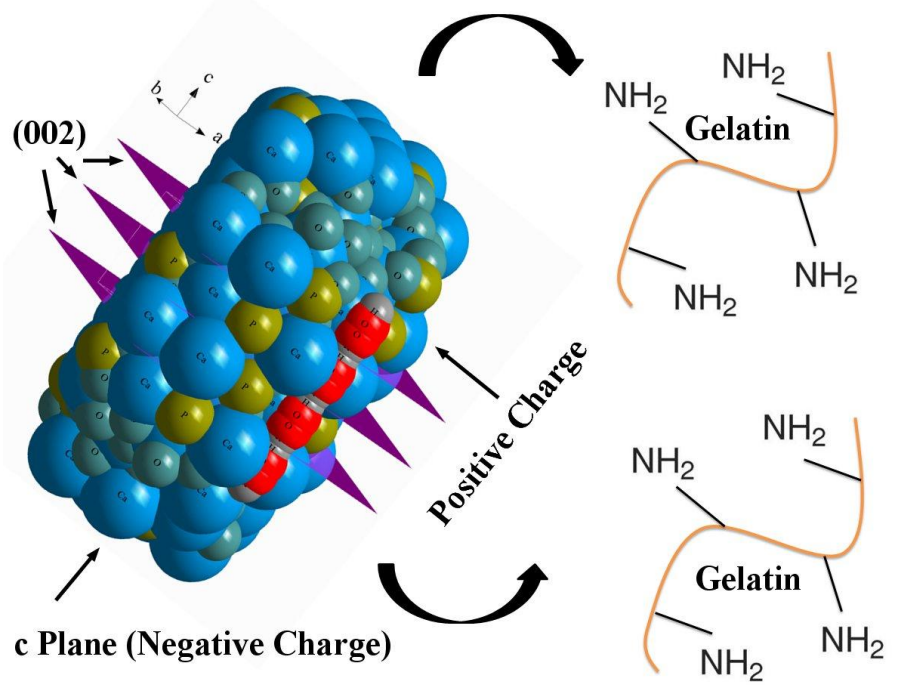

Schematic 1: Interaction between HA and gelatin

Figure 4 shows the photo and FESEM images of gelatin-HA scaffold. The presence of HA particles causes the pores to stretch and the pores are not spherical. On the scaffolds, there are bubbles of 200 micrometers in diameter that are formed by the attachment of smaller pores. HA particles enhance the accuracy of the designed pores. The HA particles are likely to influence the rheology of the gels, and with the stability of all 3D-printer factors, the scaffold structure's accuracy is improved [35].

Schematic 1 shows the Interaction between HA and gelatin schematically. (002) planes have a negative charge and (300) planes have a positive charge in HA crystals. Gelatin molecules bind to these crystals and alter the rheology of the gel (The stronger this connection, the better the mechanical properties of the scaffold).

Figure 5 shows the photo and FESEM images of gelatin-HA-rGO scaffold. The pores in this scaffold are much smaller than in the previous samples (The pores are spherical). Also, the accuracy of the design pores is better than the previous ones. In this sample, the presence of graphene sheets has again altered the gel rheology, resulting in spherical porosities, and the presence of graphene sheets has reduced the size of these pores. Reducing the size of these porosities increases the accuracy of the designed porosities [35]. Schematic 2 shows the Interaction between HA, rGO, and gelatin. The remaining agents on the graphene surface bind to the gelatin molecules, while the interface between HA and graphene is coherent. Thus, a three-way interconnection occurs between the three phases. These joints have increased mechanical properties.

Figure 6 shows the crack analysis caused by bending of scaffolds. As a result of the bending of the scaffolds, the cracks created in the gelatin-HA scaffold grow in a way that the resulting cracks are smaller than the cracks created in the pure gelatin scaffold and are moved to the corner of the scaffold. These changes in the shape of the cracks are also noticeable in the case of the gelatin-HA-rGO scaffold, which the crack is smaller and more inclined toward the corner than other scaffolds. These findings indicate that the presence of graphene and HA increased the bending resistance of the scaffolds. The findings of this study, along with other published researches, will be useful in the development of tissue engineering [40-45].

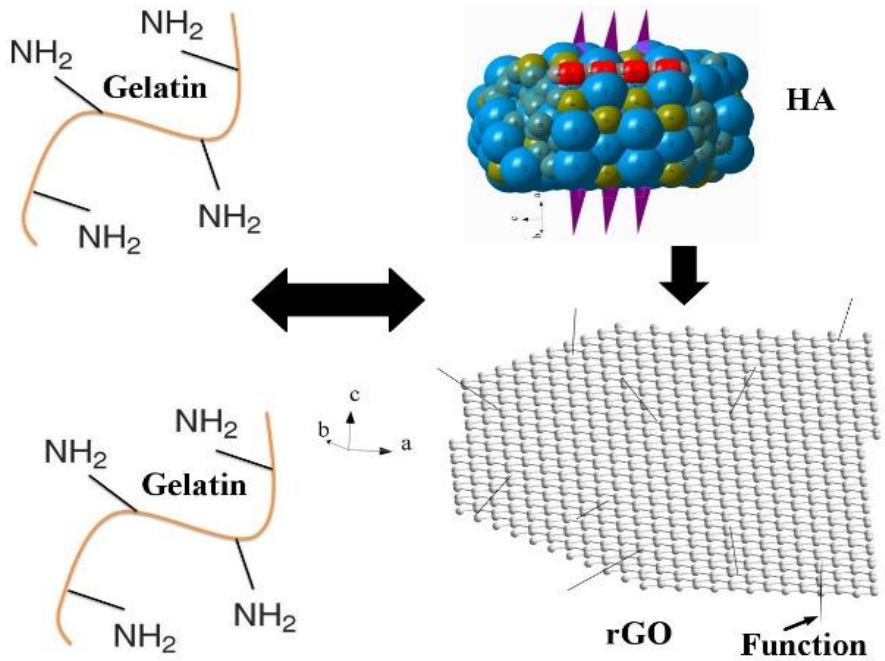

Schematic 2: Interaction between HA, rGO, and gelatin

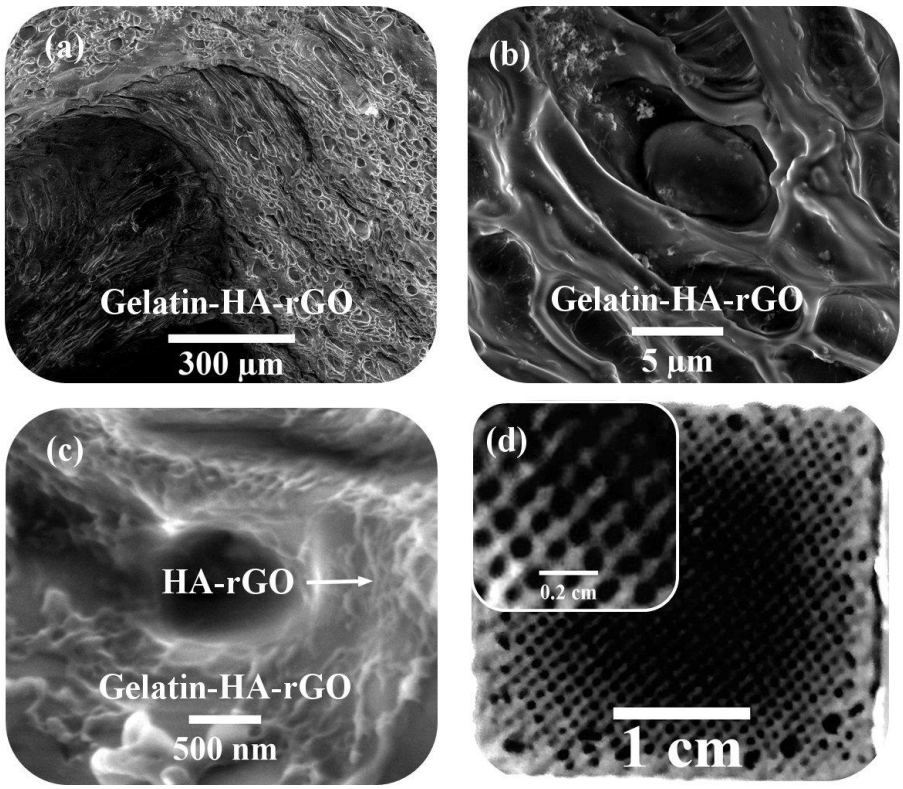

Figure 5: (a-c) FESEM images of gelatin-HA-rGO scaffold, (d) gelatin-HA-rGO scaffold photo

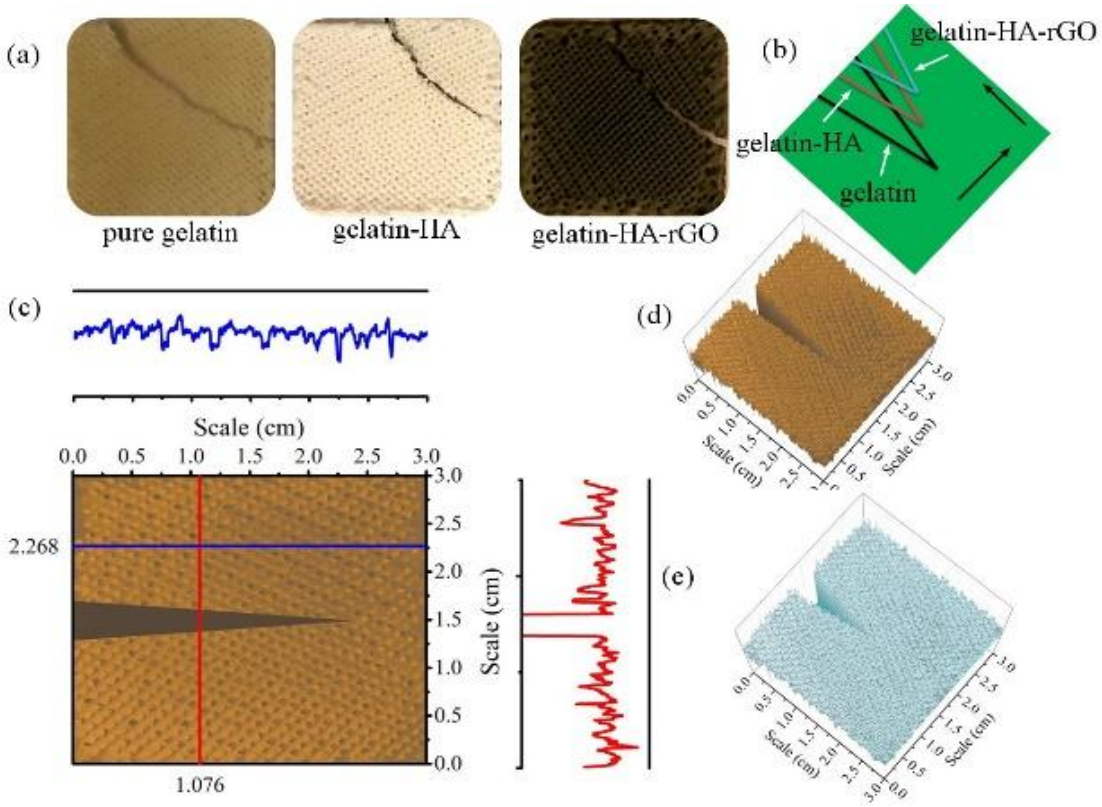

Figure 6: Crack analysis caused by bending of scaffolds

4. Conclusion

The findings of this study showed that the addition of graphene and HA to gelatin changed the rheology, reduced the size of pores, and increased the accuracy of the designed pores. The addition of HA and graphene also increased the bending strength and changed the shape of the resulting cracks. The findings of this study will be useful for the design of tissue engineering scaffolds.

Conflict of Interests

The authors certify that they have no affiliations with or involvement in any organization or entity with any financial interest, or non-financial interest in the subject matter or materials discussed in this manuscript.

Acknowledgements

No Applicable.

References

[1] M. Li, P. Xiong, F. Yan, S. Li, C. Ren, Z. Yin, et al, An overview of graphene-based hydroxyapatite composites for orthopedic applications, Bioactive Materials 3 (1) (2018) 1-18, https://doi.org/10.1016/j.bioactmat.2018.01.001

[2] Y. Qu, F. He, C. Yu, X. Liang, D. Liang, L. Ma, et al, Advances on graphene-based nanomaterials for biomedical applications, Materials Science & Engineering C 90 (2018) 764–780, https://doi.org/10.1016/j.msec.2018.05.018

[3] C. Nie, L. Ma, S. Li, X. Fan, Y. Yang, C. Cheng, W. Zhao, C. Zhao, Recent progresses in graphene based bio-functional nanostructures for advanced biological and cellular interfaces, Nanotoday 26 (2019) 57-97, https://doi.org/10.1016/j.nantod.2019.03.003

[4] S. Gadipelli, Z. X. Guo, Graphene-based materials: Synthesis and gas sorption, storage and separation, Progress in Materials Science 69 (2015) 1–60, http://dx.doi.org/10.1016/j.pmatsci.2014.10.004

[5] M. D. Stolle, S. Park, Y. Zhu, J. An, R. S. Ruoff, Graphene-based ultracapacitors, Nano Lett. 8 (10) (2008) 3498–3502, https://doi.org/10.1021/nl802558y

[6] J. Liu, J. Dong, T. Zhang, Q. Peng, Graphene-based nanomaterials and their potentials in advanced drug delivery and cancer therapy, Journal of Controlled Release 286 (2018) 64-73, https://doi.org/10.1016/j.jconrel.2018.07.034

[7] N. A. Hussien, N. klan, M.Türk, Aptamer-functionalized magnetic graphene oxide nanocarrier for targeted drug delivery of paclitaxel, Materials Chemistry and Physics 211 (2018) 479-488, https://doi.org/10.1016/j.matchemphys.2018.03.015

[8] E. Paz, F. Forriol, J. C. del Real, N. Dunne, Graphene oxide versus graphene for optimisation of PMMA bone cement for orthopaedic applications, Materials Science and Engineering: C 77 (2017) 1003-1011, https://doi.org/10.1016/j.msec.2017.03.269

[9] J. Lin, X. Chen, P. Huang, Graphene-based nanomaterials for bioimaging, Advanced Drug Delivery Reviews, Part B 105 (2016) 242-254, https://doi.org/10.1016/j.addr.2016.05.013

[10] D. Lahiri, S. Ghosh, A. Agarwal, Carbon nanotube reinforced hydroxyapatite composite for orthopedic application: a review, Mater Sci Eng C 32 (7) (2012) 1727–1758, https://doi.org/10.1016/j.msec.2012.05.010

[11] D. Li, X. Xie, Z. Yang, C. Wang, Z. Wei, P. Kang, Enhanced bone defect repairing effects in glucocorticoid-induced osteonecrosis of the femoral head using a porous nano-lithium-hydroxyapatite/gelatin microsphere/erythropoietin composite scaffold, Biomater. Sci. 6 (2018) 519-537, https://doi.org/10.1039/C7BM00975E

[12] H. Nosrati, D. Q. S. Le, R. Z. Emameh, C. E. Bunger, Characterization of the precipitated Dicalcium Phosphate Dehydrate on the Graphene Oxide surface as a bone cement reinforcement, Journal of Tissues and Materials 2 (1) (2019) 33-46, DOI: 10.22034/jtm.2019.173565.1013

[13] Z. Qin, A. Gautieri, A.K. Nair, H. Inbar, M.J. Buehler, Thickness of Hydroxyapatite Nanocrystal Controls Mechanical Properties of the Collagen Hydroxyapatite Interface, Langmuir 28 (4) (2012) 1982-1992, https://doi.org/10.1021/la204052a

[14] H. Nosrati, N. Ehsani, H. Baharvandi, M. Mohtashami, H. Abdizadeh, V. Mazinani, Effect of primary materials ratio and their stirring time on SiC nanoparticle production efficiency through sol-gel process, American Journal of Engineering Research (AJER) 3

(3) (2014) 317-321

[15] H. Nosrati, M. S. Hosseini, M. Nemati, A. Samariha, Production of TiO2 Nano-Rods Using Combination of Sol-Gel and Electrophoretic Methods, Asian Journal of Chemistry 25 (6) (2013) 3484-3486, http://dx.doi.org/10.14233/ajchem.2013.14250

[16] H. Nosrati, N. Ehsani, H.R. Baharvandi, H. Abdizadeh, Effect of pH on Characteristics of SiC Nanoparticles and Production Efficiency Using Chemical Method, American-Eurasian J. Agric. & Environ. Sci., 12 (5) (2012) 674-677

[17] H. Nosrati, R. Sarraf Mamoory, D. Q. S. Le, C. E. Bunger, R. Zolfaghari Emameh, F. Dabir, Gas injection approach for synthesis of hydroxyapatite nanorods via hydrothermal method, Materials Characterization 2019; 110071, https:// doi.org/10.1016/ j.matchar. 2019.110071

[18] M. Canillas, R. Rivero, R. García-Carrodeguas, F. Barba, M.A. Rodríguez, Processing of hydroxyapatite obtained by combustion synthesis, Boletín de la Sociedad Española de Cerámica y Vidrio 56 (5) (2017) 237-242, https://doi.org/10.1016/j.bsecv.2017.05.002

[19] X. Guo, H. Yan, S. Zhao, L. Zhang, Y. Li, X. Liang, Effect of calcining temperature on particle size of hydroxyapatite synthesized by solid-state reaction at room temperature, Advanced Powder Technology 4 (6) (2013) 1034-1038, https://doi.org/10.1016/j.apt.2013.03.002

[20] M. Shikhanzadeh, Direct formation of nanophase hydroxyapatite on cathodically polarized electrodes., J Mater Sci: Mater Med. 9 (1998) 67-72, http://dx.doi.org/10.1023/A:1008838813120

[21] A. Jillavenkatesa, R.A. Condrate Sr., Sol–gel processing of hydroxyapatite, J. Mater. Sci. 33 (1998) 4111–4119, https://doi.org/10.1023/A:1004436732282

[22] T.A. Kuriakosea, S.N. Kalkura, M. Palanichami, D. Arivuoli, K. Dierks, G. Bocelli, C. Betzel, Synthesis of stoichiometric nano crystalline hydroxyapatite by ethanol-based sol–gel technique at low temperature, Journal of Crystal Growth 263 (1-4) (2004) pp. 517-523, https://doi.org/10.1016/j.jcrysgro.2003.11.057

[23] O. V. Sinitsyna, A. G. Veresov, E. S. Kovaleva, Y. V. Kolen'ko, V. L. Putlyaev, Y. D. Tretyakov, Synthesis of hydroxyapatite by hydrolysis of α-Ca3(PO4)2, Russian Chemical Bulletin 54 (1) (2005) 79-86, https://doi.org/10.1007/s11172-005-0220-9

[24] Liu, Y. Huang, W. Shen, J. Cui, Kinetics of hydroxyapatite precipitation at pH 10 to 11, Biomaterials 22 (4) (2000) 301-306, https://doi.org/10.1016/S0142-9612(00)00166-6

[25] C.M. Manuel, M.P. Ferraz, F.J. Monteiro, Synthesis of hydroxyapatite and tri calcium phosphate nanoparticles Preliminary Studies, Key Eng Mater. 240-242 (2003) 555-558, https://doi.org/10.4028/www.scientific.net/KEM.240-242.555

[26] K. Yamashita, T. Arashi, K. Kitagaki, S. Yamada, T. Umegaki, Preparation of apatite thin films through rfsputtering from calcium phosphate glasses, J. Am. Ceram. Soc. 77 (9) (1994) 2401–2407, https://doi.org/10.1111/j.1151-2916.1994. tb04611.x

[27] Kimura, Synthesis of hydroxyapatite by interfacial reaction in a multiple emulsion, Res Lett Mater Sci. (2007) 1-4, http://dx.doi.org/10.1155/2007/71284

[28] A.C. Tas, Synthesis of biomimetic Ca-hydroxyapatite powders at 37 degrees C in synthetic body fluids, Biomaterials 21 (2000) 1429-1438, http://dx.doi.org/10.1016/S0142-9612(00)00019-3

[29] C. Qi, Y-J Zhu, G-J Ding, J. Wu, F. Chen, Solvothermal synthesis of hydroxyapatite nanostructures with various morphologies using adenosine 50-monophosphate sodium salt as an organic phosphorus source, RSC Adv. 5 (2015) 3792-3798, DOI: 10.1039/c4ra13151g

[30] I.S. Neira, Y.V. Kolen'ko, O.I. Lebedev, G. Van Tendeloo, H.S. Gupta, F. Guitián, M. Yoshimura, An Effective Morphology Control of Hydroxyapatite Crystals via Hydrothermal Synthesis, Cryst. Growth Des. 9 (1) (2009) 466-474, https://doi.org/10.1021/cg800738a

[31] Nosrati, R. Sarraf-Mamoory, F. Dabir, Crystallographic study of hydrothermal synthesis of hydroxyapatite nano-rods using Brushite precursors, Journal of Tissues and Materials 2 (3) (2019) 1-8, DOI: 10.22034/jtm.2019.199830.1022

[32] H. Nosrati, R. Sarraf-Mamoory, D. Q. S. Le, C. E. Bunger, Preparation of reduced graphene oxide/hydroxyapatite nanocomposite and evaluation of graphene sheets/hydroxyapatite interface, Diamond & Related Materials 100 (2019) 107561,

https://doi.org/10.1016/j.diamond.2019.107561

[33] H. Nosrati, R. Sarraf Mamoory, F. Dabir, M. C. Perez M. A. Rodriguez, D. Q. S. Le, C. E. Bünger, In situ synthesis of three dimensional graphene/hydroxyapatite nano powders via hydrothermal process, Materials Chemistry and Physics 222 (2019) 251–255, https://doi.org/10.1016/j.matchemphys.2018.10.023

[34] H. Nosrati, R. Sarraf Mamoory, F. Dabir, D. Q. S. Le, C. E. Bunger, M. C. Perez, M. A. Rodriguez, Effects of hydrothermal pressure on in situ synthesis of 3D graphene/hydroxyapatite nano structured powders, Ceramics International 45 (2019) 1761–1769, https://doi.org/10.1016/j.ceramint.2018.10.059

[35] H. Nosrati, R. Sarraf-Mamoory, D. Q. S. Le, C. E. Bunger, Fabrication of gelatin/hydroxyapatite/3D-graphene scaffolds by a hydrogel 3D-printing method, Materials Chemistry and Physics 239 (2020) 122305, https://doi.org/10.1016/j.matchemphys.2019.122305

[36] A. H. Ahmadi, H. Nosrati, R. Sarraf-Mamoory, Decreasing β- three calcium phosphate particle size using graphite as nucleation sites and diethylene glycol as a chemical additive, Journal of Bioengineering Research 1(4) (2020), DOI:10.22034/JBR.2019.211371.1016

[37] H. Nosrati, R. Sarraf-Mamoory, D.Q.S. Le, M. Canillas Perez, C. Bunger, Studying the physical behavior of human mesenchymal stem cells on the surface of hydroxyapatite after adding graphene as a reinforcement, Journal of Bioengineering Research (2020), doi: 10.22034/jbr.2019.213164.1018

[38] S. Baradaran, E. Moghaddam, W.J. Basirun, M. Mehrali, M. Sookhakian, M. Hamdi, et al, Mechanical properties and biomedical application of a nanotube hydroxyapatite-reduced graphene oxide composite, Carbon 69 (2014) 32–45, http://dx.doi.org/10.1016/j.carbon.2013.11.054.

[39] H. Nosrati, R. Sarraf-Mamoory, D.Q.S. Le, C.E. Bünger, Enhanced fracture toughness of three dimensional graphene- hydroxyapatite nanocomposites by employing the Taguchi method, Composites Part B: Engineering 190 (2020) 107928; https://doi.org/10.1016/j.compositesb.2020.107928

[40] H. Nosrati, R. Sarraf-Mamoory, D.Q.S. Le, M.C. Perez, C.E. Bünger, Evaluation of Argon-Gas-Injected Solvothermal Synthesis of Hydroxyapatite Crystals Followed by High-Frequency Induction Heat Sintering, Cryst. Growth Des. 20(5) (2020) 3182-3189; https://doi.org/10.1021/acs.cgd.0c00048

[41] H. Nosrati, R. Sarraf-Mamoory, A.H. Ahmadi, M.C. Perez, Synthesis of Graphene Nanoribbons–Hydroxyapatite Nanocomposite Applicable in Biomedicine and Theranostics, J. Nanotheranostics 1(1) (2020) 2; https://doi.org/10.3390/jnt1010002

[42] A. Aidun, A.S. Firoozabady, M. Moharrami, A. Ahmadi, N. Haghighipour, S. Bonakdar, Graphene oxide incorporated polycaprolactone/chitosan/collagen electrospun scaffold: Enhanced osteogenic properties for bone tissue engineering, Artifical Organs 43(10) (2019) 264-281; https://doi.org/10.1111/aor.13474

[43] F. Ghorbani, A. Zamanian, A. Shams, A. Shamoosi, A. Aidun, Fabrication and characterisation of super-paramagnetic responsive PLGA–gelatine–magnetite scaffolds with the unidirectional porous structure: a physicochemical, mechanical, and in vitro evaluation, IET Nanobiotechnology 13(8) (2019) 860 – 867; https://doi.org/10.1049/iet-nbt.2018.5305

[44] H.Z. Marzouni, F. Tarkhan, A. Aidun, K. Shahzamani, H.R. Jahan Tigh, S. Malekshahian, H.E. Lashgarian, Cytotoxic Effects of Coated Gold Nanoparticles on PC12 Cancer Cell, Galen Medical Journal 7 (2018); http://dx.doi.org/10.22086/gmj.v0i0.1110

[45] A. Aidun, A. Zamanian, F. Ghorbani, Immobilization of polyvinyl alcohol-siloxane on the oxygen plasma-modified polyurethane-carbon nanotube composite matrix, Applied Polymer 137(12) (2020) 48477; https://doi.org/10.1002/app.48477